

## Electronic Supplementary Information

### Double-sided engineering for space-confined reversible Zn anode

Yong Gao<sup>1,2,4</sup>, Nute Yang<sup>1,2,4</sup>, Fan Bu<sup>1,2,4</sup>, Qinghe Cao<sup>1,2</sup>, Jie Pu<sup>1,3</sup>, Yuxuan Wang<sup>1</sup>, Ting Meng<sup>1</sup>,  
Jipeng Chen<sup>1</sup>, Wenbo Zhao<sup>1</sup>, Cao Guan<sup>1,2\*</sup>

<sup>1</sup>Institute of Flexible Electronics, Northwestern Polytechnical University, Xi'an 710072, China.

<sup>2</sup>Key laboratory of Flexible Electronics of Zhejiang Province, Ningbo Institute of Northwestern Polytechnical University, 218 Qingyi Road, Ningbo, 315103, China.

<sup>3</sup>School of Electrical and Electronic Engineering, Nanyang Technological University, Singapore 639798, Singapore.

<sup>4</sup>These authors contribute equally: Yong Gao, Nute Yang, Fan Bu.

Corresponding Authors

\*E-mail: iamcguan@nwpu.edu.cn (C. Guan)

## **Methods**

### **Preparation of ZnS/Zn/Cu electrode**

The ZnS/Zn/Cu electrode was prepared by magnetron sputtering method. First, the 10  $\mu\text{m}$  zinc foil was sandpapered and sonicated in alcohol. Then, Zn/Cu electrode was prepared using a DC target with a power of 25 W, Ar gas with a flow rate of 30 sccm, and held for 10 mins. Finally, ZnS was sputtered on the top surface of the pre-obtained Zn/Cu electrode using an RF target with a power of 50 W, Ar gas with a flow rate of 40 sccm, and held for 15 mins. Zn/Cu and ZnS/Zn electrodes are obtained by only sputtering Cu or ZnS on the Zn foil.

### **Preparation of NVO cathode materials**

NVO nanowires were synthesized by a hydrothermal method. Specifically, 4 mmol  $\text{V}_2\text{O}_5$  and 4 mmol NaOH were dissolved in distilled water. The volume of the solution was set to 85 mL and magnetically stirred for 1 hour at room temperature. The solution was then transferred to an autoclave and heated at 180  $^\circ\text{C}$  for 24 hours. The NVO nanowires were collected by centrifugation, washed with water and alcohol, and dried at 80  $^\circ\text{C}$  overnight. The cathode slurry consisted of NVO-activated material, polyvinylidene fluoride (PVDF) binder, and Super P conductive agent (7:1.5:1.5 by weight). Finally, the slurry was coated onto a titanium foil and vacuum-dried overnight at 60 $^\circ\text{C}$  (loading masses of  $\sim 0.8 \text{ mg cm}^{-2}$  and  $\sim 10 \text{ mg cm}^{-2}$ ).

### **Materials characterization**

Field emission scanning electron microscopy (FE-SEM) dates were conducted using FEI Verios G4 (20 kV). XPS spectra were tested from Kratos (Axis Supra). XRD studies were obtained using Bruker D8 Advanced with radiation from a Cu target. Focused ion beam (FIB) etching was realized using FEI Helios G4 CX (30 kV) equipped with an Energy dispersive spectrometer (EDS)

(Thermofisher, Thermo NS7). Thermal conductivity coefficient was tested with Hot Disk TPS2200 thermal constant analyzer (AB Co., Sweden). The tensile tests were tested on a universal testing machine (INSTRON 3344) with a sample size of  $0.5 \times 4 \text{ cm}^2$ . Four-probe resistance results were obtained from tester H7756.

### **Finite element simulation**

To simulate local temperature, 3D model was constructed using COMSOL Multiphysics software, and the whole model is  $10 \text{ }\mu\text{m} \times 10 \text{ }\mu\text{m} \times 10 \text{ }\mu\text{m}$  cube in size. The thermal conductivity of Zn/Cu is approximately twice that of bare Zn according to the experiment, and the calculated transient time is  $4 \times 10^{-5} \text{ s}$ . The stress distribution and electrode current density were simulated using a simplified 2D model. The stress distribution was determined using the solid mechanics module, the shape of electrode was determined by experimental results, and a pre-strain of 0.1 was used for the boundary conditions. Meanwhile, the AC/DC model was used to simulate current density with boundary condition of  $5 \text{ mA cm}^{-2}$ .

### **Molecular dynamics (MD) simulations**

Zn and Zn/Cu were modeled with the same force field. The Lammmps package was used for MD simulations. The integration of the equations of motion is performed using the Verlet frog jump algorithm with a time step of 1 fs. The initial and final temperatures were set to 300 K and the pressures in the X and Y directions were controlled. Periodic boundary conditions were applied along the X and Y directions and free boundary conditions were used in the stretching direction.

### **Electrochemical measurement**

All electrochemical tests were performed at room temperature. The prepared electrode was cut into discs (diameter 12 mm) as anode. For electrochemical tests, CR-2032 type coin cells were

assembled using glass fiber filter (GF-A, Whatman) as the separator. Symmetrical cells using 2 M ZnSO<sub>4</sub> electrolyte were used to study the Zn deposition behavior. **The coin-cell sealing pressure is 5 MPa.** To study coulombic efficiency, asymmetrical cells were assembled using Cu foil as the work electrode, ZnS/Zn/Cu as the anode and 2 M ZnSO<sub>4</sub> as the electrolyte, and the stripping cutoff voltage was set at 0.5 V (vs. Zn<sup>2+</sup>/Zn). For the full battery's tests, 2 M ZnSO<sub>4</sub> was used as the electrolyte. The capacities of the full cells were obtained based on the weight of NVO active materials. All the controlled samples, including bare Zn, Zn/Cu, ZnS/Zn and ZnS/Zn/Cu electrodes, were investigated in the same condition.

The specific energy density and volumetric energy density of full cell is calculated by the following equations:

$$E_m = \frac{\int IU dt}{m} \quad (S1)$$

$$E_v = \frac{\int IU dt}{V} \quad (S2)$$

where  $E_m$  is the specific energy density,  $E_v$  represents the volumetric energy density,  $U$  is discharging voltage,  $I$  is the discharging current,  $dt$  represents the time differential,  $m$  refers to the whole mass of electrodes, and  $V$  refers to the whole volume of the cell.

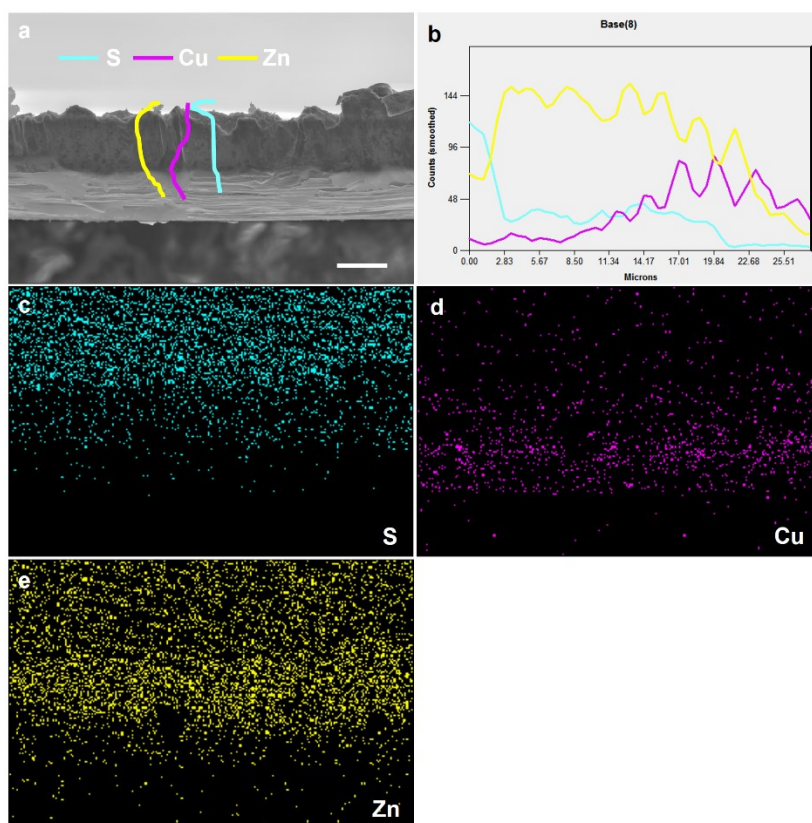


**Fig S1** (a) Cross-section SEM image with (b) the corresponding EDS line-scan results of ZnS/Zn/Cu electrode. The element mapping for (c) S, (d) Cu and (e) Zn of Fig S1(a). Scale bar, 10  $\mu\text{m}$ .

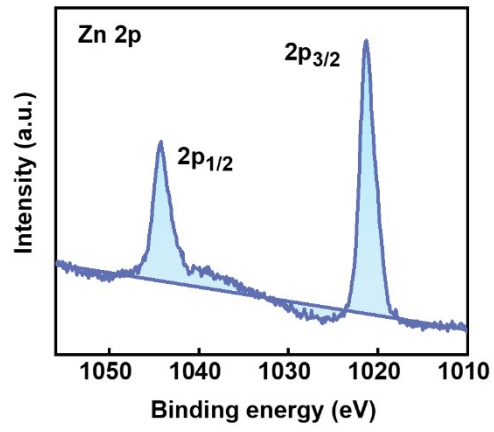
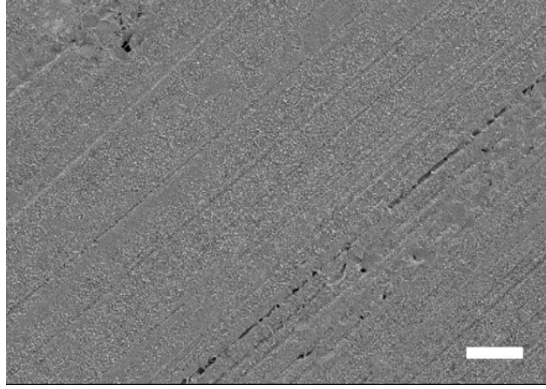
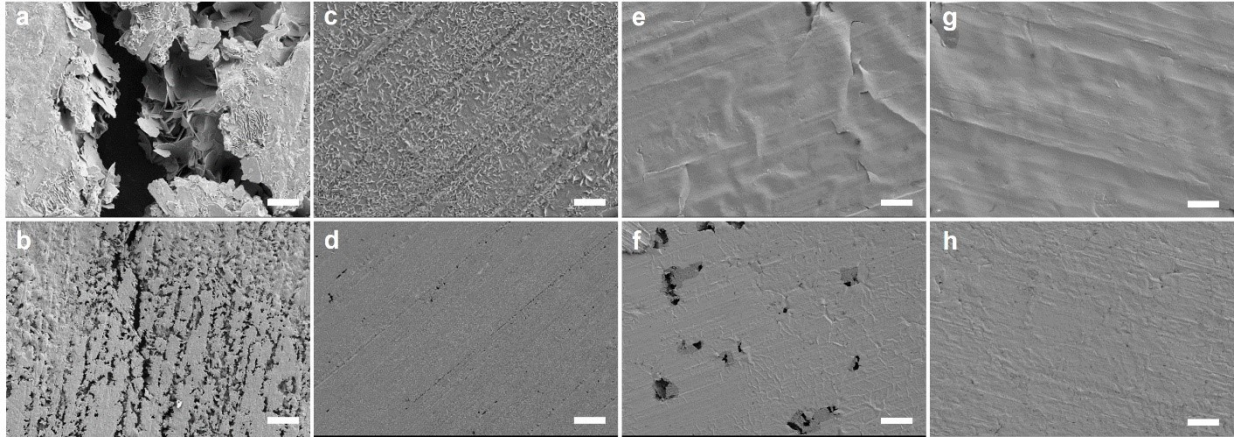


Fig S2 XPS pattern of Zn element of the top layer.



**Fig S3** SEM images of Zn stripping from bare Zn/Cu electrode with a capacity of  $3 \text{ mAh cm}^{-2}$  at  $5 \text{ mA cm}^{-2}$ . Scale bar,  $20 \mu\text{m}$ .



**Fig S4** SEM images of Zn stripping from (a, b) bare Zn, (c, d) Zn/Cu, (e, f) ZnS/Zn, and (g, h) ZnS/Zn/Cu electrodes with a capacity of  $3 \text{ mAh cm}^{-2}$  at  $5 \text{ mA cm}^{-2}$ . Scale bar,  $5 \mu\text{m}$  for a, c, e and g,  $50 \mu\text{m}$  for b, d, f and h.



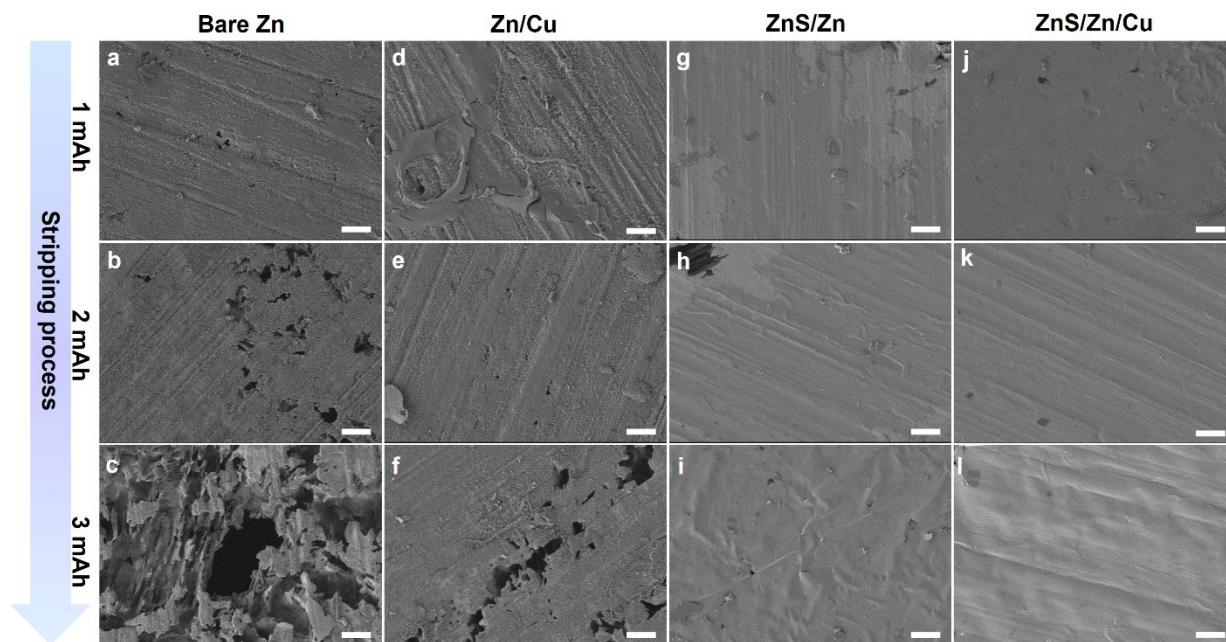


**Fig S5** SEM images of Zn stripping process from (a, b, c) bare Zn, (d, e, f) Zn/Cu, (g, h, i) ZnS/Zn, and (j, k, l) ZnS/Zn/Cu electrodes with capacities from 1 to 3 mAh cm<sup>-2</sup> at 5 mA cm<sup>-2</sup>. Scale bar, 10 μm.

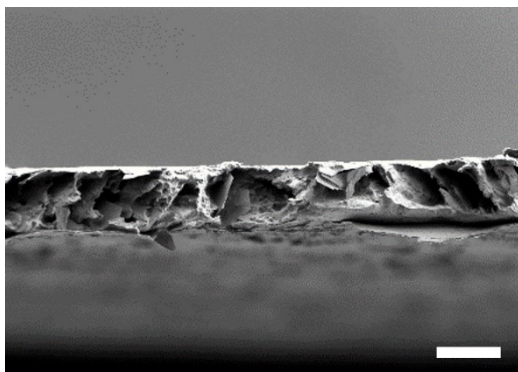


**Fig S6** Cross-section SEM image of the Zn/Cu electrode after 10 cycles with a capacity of  $5 \text{ mAh cm}^{-2}$  at  $5 \text{ mA cm}^{-2}$ . Scale bar,  $10 \text{ }\mu\text{m}$ .

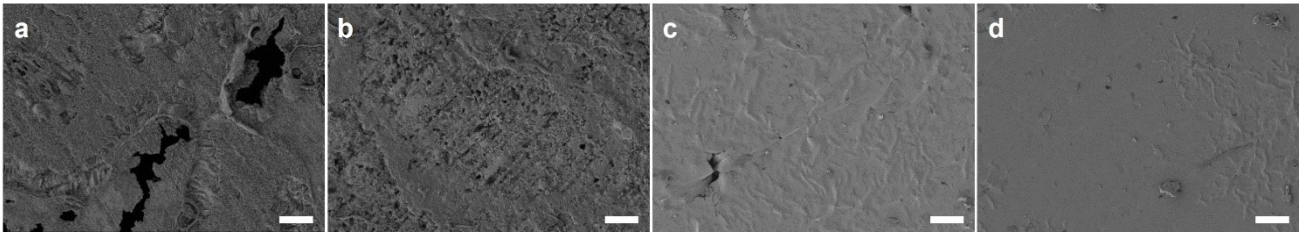


**Fig S7** SEM images of Zn stripping/plating on (a) bare Zn, (b) Zn/Cu, (c) ZnS/Zn, and (d) ZnS/Zn/Cu electrodes after 10 cycles with a capacity of  $5 \text{ mAh cm}^{-2}$  at  $5 \text{ mA cm}^{-2}$ . Scale bar,  $20 \mu\text{m}$ .

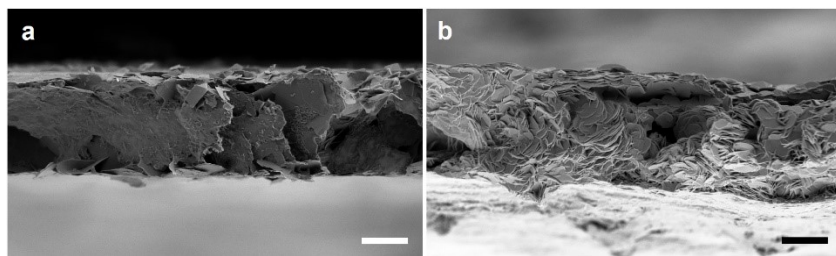


**Fig S8** High magnification cross-section SEM images of (a) ZnS/Zn and (b) ZnS/Zn/Cu electrodes after 10 cycles with 5 mAh cm<sup>-2</sup>/5 mA cm<sup>-2</sup>. Scale bar, 5 μm.

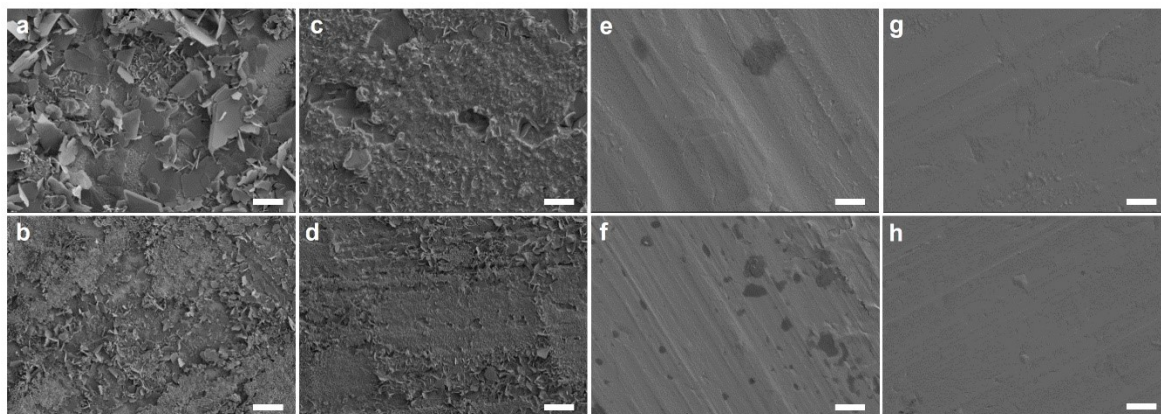


**Fig S9** SEM images of Zn deposition on (a, b) bare Zn, (c, d) Zn/Cu, (e, f) ZnS/Zn, and (g, h) ZnS/Zn/Cu electrodes with a capacity of  $3 \text{ mAh cm}^{-2}$  at  $5 \text{ mA cm}^{-2}$ . Scale bar,  $2 \mu\text{m}$  for a, c, e and g,  $10 \mu\text{m}$  for b, d, f and h.

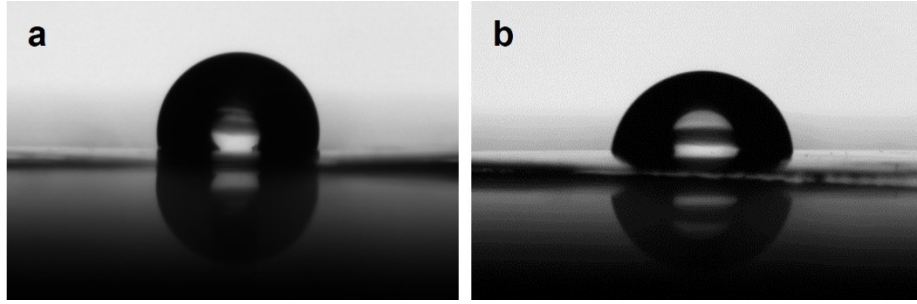


**Fig S10** Contact angles of 2M ZnSO<sub>4</sub> aqueous solution on (a) bare Zn and (b) ZnS/Zn/Cu electrodes.

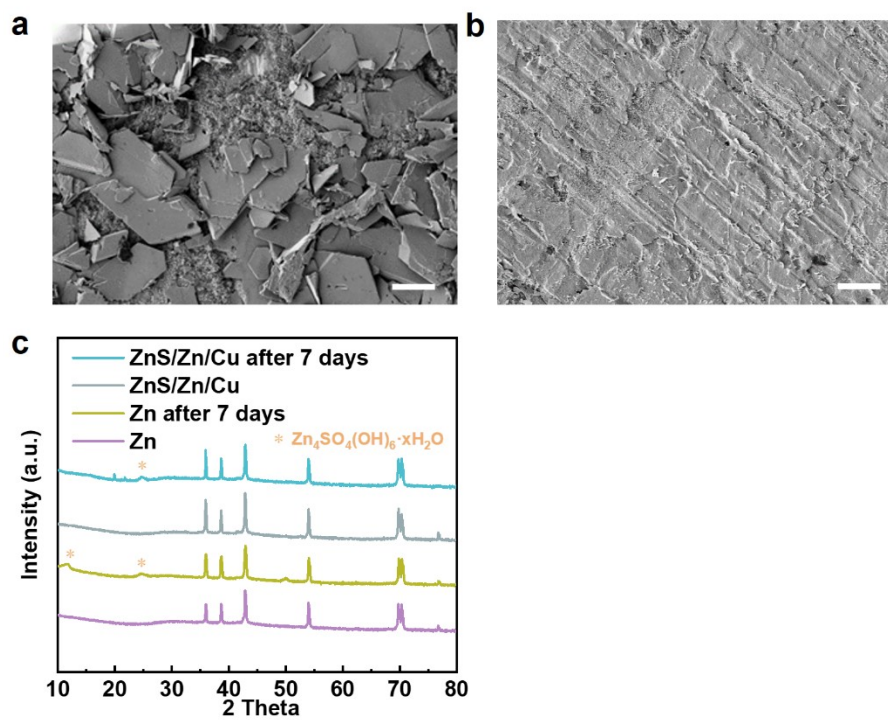


**Fig S11** SEM images of (a) bare Zn and (b) ZnS/Zn/Cu electrodes that immersed in 2M ZnSO<sub>4</sub> electrolyte for 7days. (c) The corresponding XRD curves. Scale bar, 10 μm for a and b.

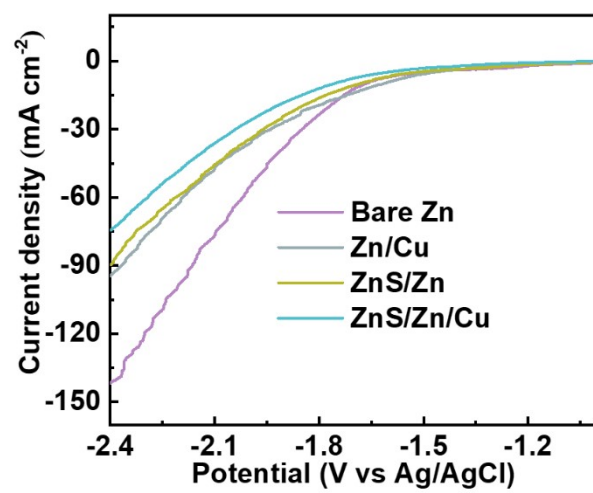
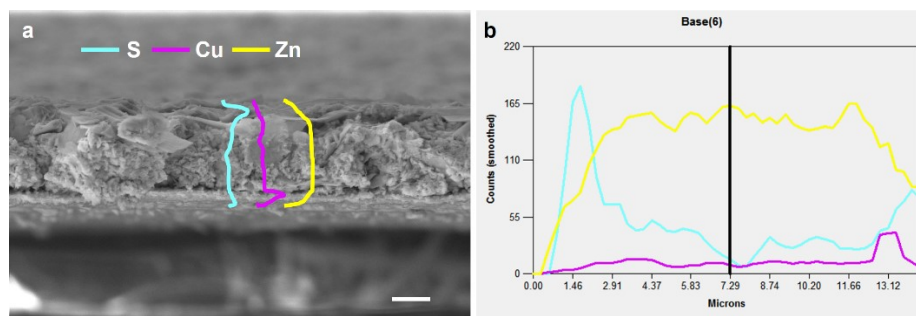
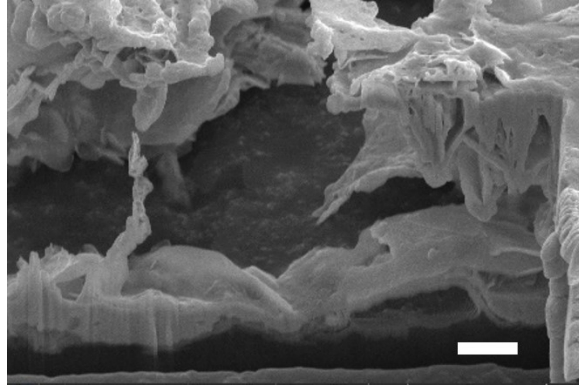


Fig S12 HER curves of different electrodes.





**Fig S13 (a)** Cross-sectional SEM image and **(b)** the corresponding EDX line-scan results of ZnS/Zn/Cu after cycling for 10 cycles. Scale bar, 5  $\mu\text{m}$ .



**Fig S14** FIB-SEM image of bare Zn electrode after Zn stripping at  $5 \text{ mAh cm}^{-2}/5 \text{ mA cm}^{-2}$ . Scale bar,  $2 \mu\text{m}$ .

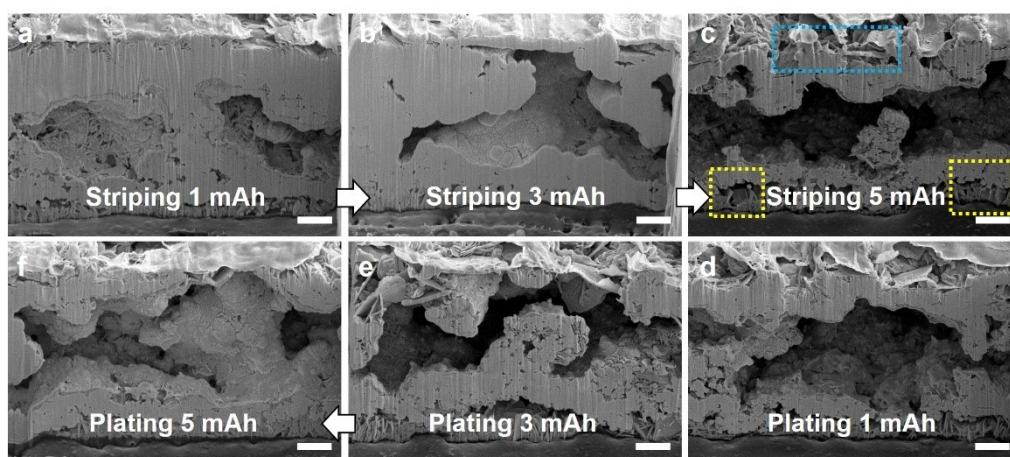


**Fig S15** FIB-SEM images of Zn stripped with capacities of (a) 1 mAh cm<sup>-2</sup>, (b) 3 mAh cm<sup>-2</sup> and (c) 5 mAh cm<sup>-2</sup>, and then plated with (d) 1 mAh cm<sup>-2</sup>, (e) 3 mAh cm<sup>-2</sup> and (f) 5 mAh cm<sup>-2</sup> on ZnS/Zn electrode at a current density of 5 mA cm<sup>-2</sup>. Scale bar, 2 μm.

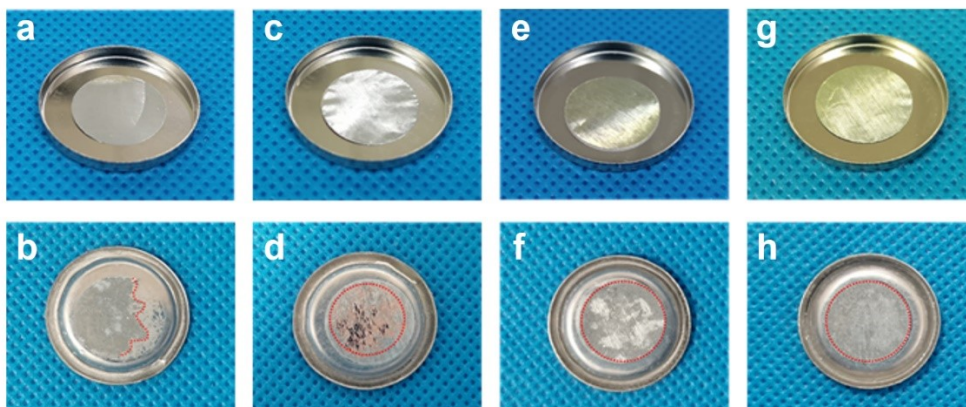


**Fig S16** Digital photos of (a, b) bare Zn, (c, d) Zn/Cu, (e, f) ZnS/Zn, and (g, h) ZnS/Zn/Cu electrodes before and after stripping with a capacity of  $5 \text{ mAh cm}^{-2}$  at  $5 \text{ mA cm}^{-2}$ . The diameter of the electrodes is 12 mm.

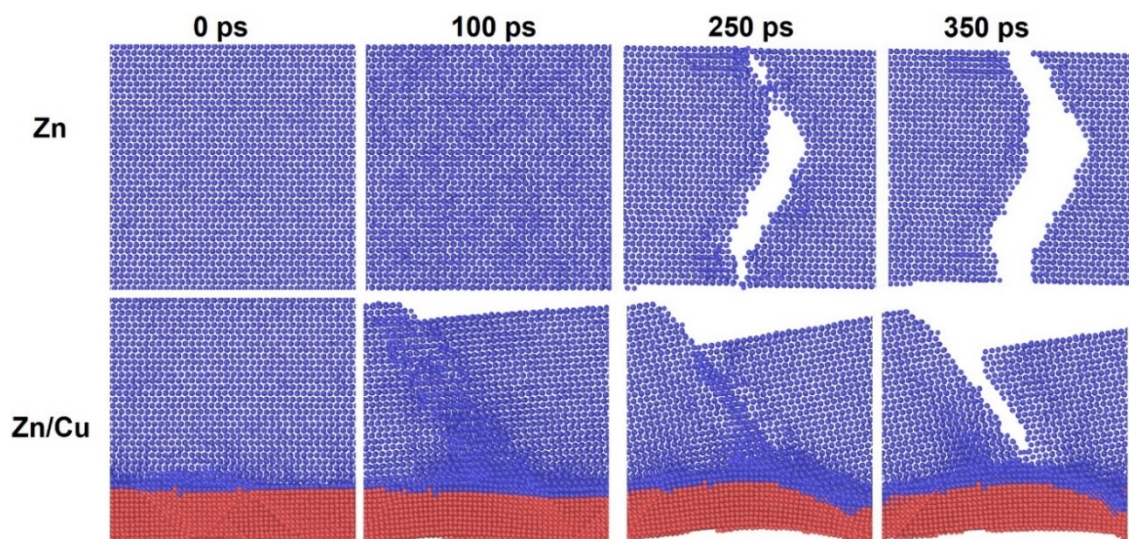


**Fig S17** MD simulation of structural evolution under stress for bare Zn and Zn/Cu electrodes at different computation times.

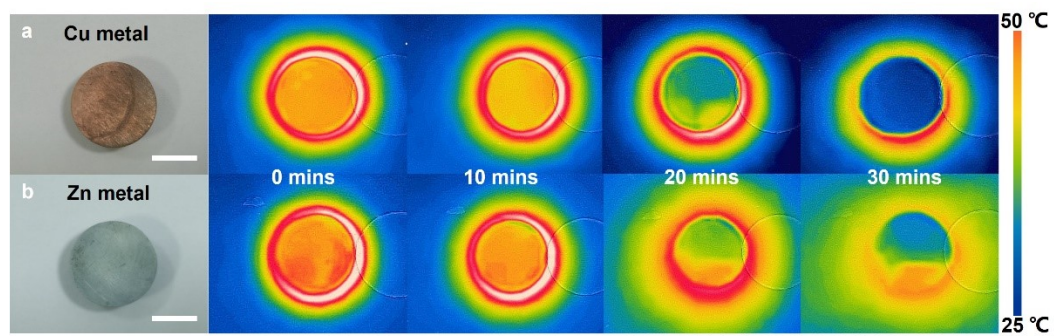


**Fig S18** Infrared thermography images of (a) Cu metal and (b) Zn metal. Scale bar, 1 cm.

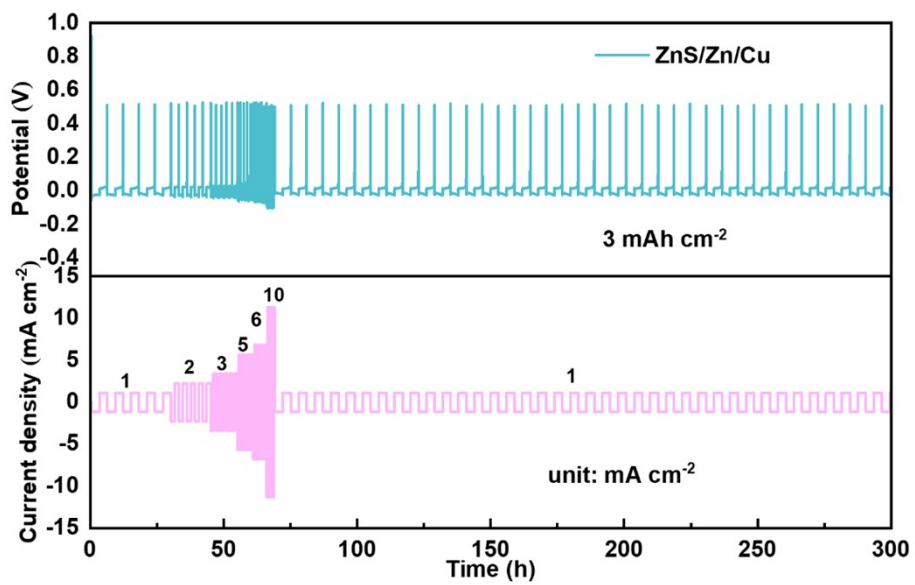
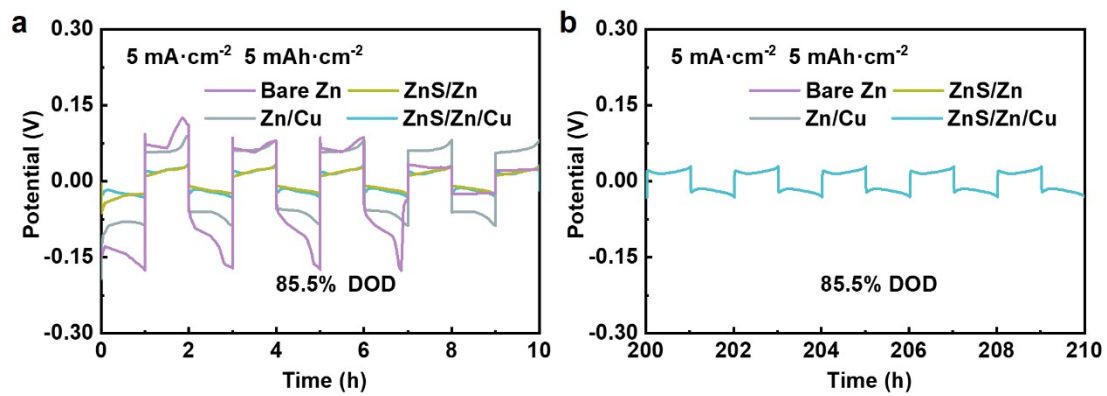
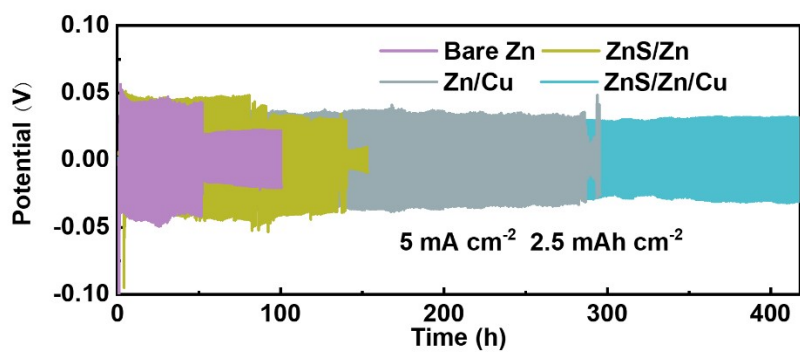


Fig S19 Cycling performance of the ZnS/Zn/Cu||Cu asymmetric cells with a capacity of 3 mAh cm<sup>-2</sup> at 1-10 mA cm<sup>-2</sup>.



**Fig S20** Cycling performance of the bare Zn, Zn/Cu, ZnS/Zn, and ZnS/Zn/Cu anodes based symmetric cells at 85.5% DOD.





**Fig S21** Cycling performance of the bare Zn, Zn/Cu, ZnS/Zn, and ZnS/Zn/Cu anodes based symmetric cells with a capacity of 2.5 mAh cm<sup>-2</sup> at 5 mA cm<sup>-2</sup>.

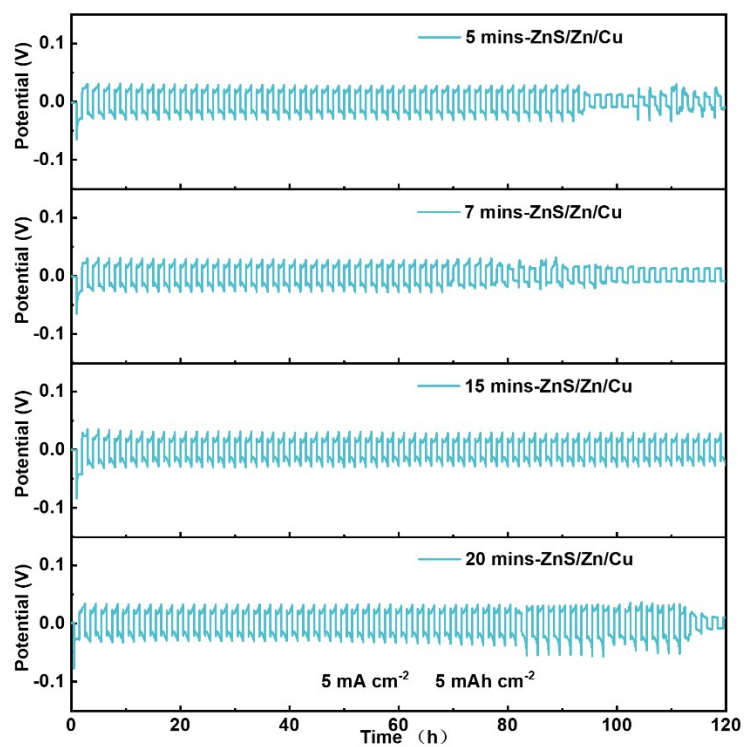


**Fig S22** Cycling performance of the ZnS/Zn/Cu anode based symmetric cells at 85.5% DOD with different thicknesses of ZnS layer.

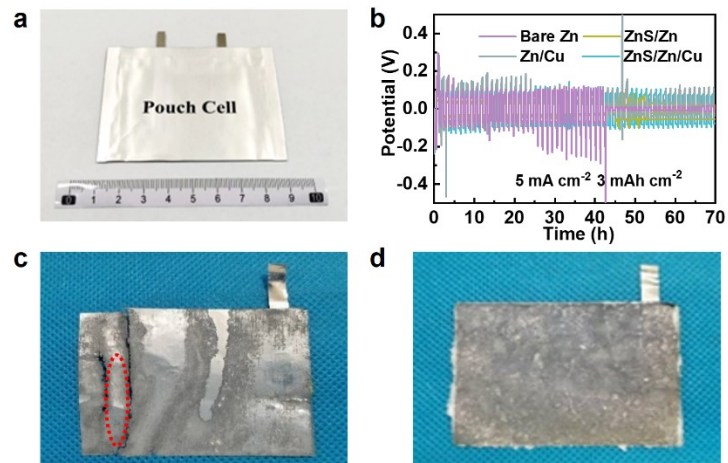


**Fig S23** (a) Digital photos of ZnS/Zn/Cu electrode based symmetrical soft pouch cell. (b) The cycling performance of different symmetrical soft pouch cells at 3 mAh cm<sup>-2</sup>/5 mA cm<sup>-2</sup>. Digital photos of (c) bare Zn and (d) ZnS/Zn/Cu electrodes after the cycling tests.

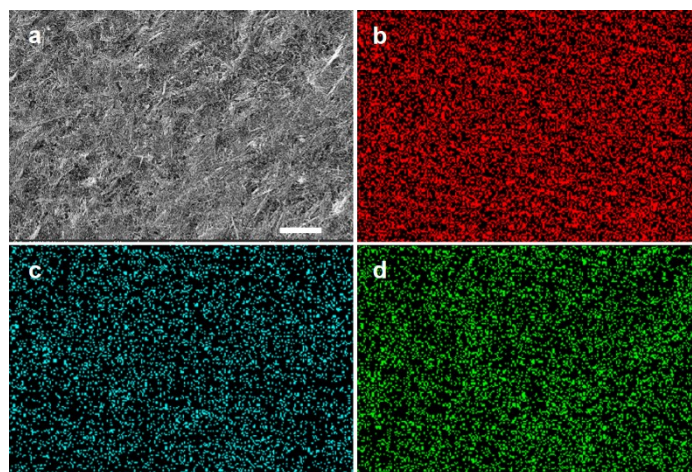


**Fig S24** (a) SEM image of NVO cathode ( $0.8 \text{ mg cm}^{-2}$ ) and the corresponding element mapping for (b) V, (c) Na and (d) O. Scale bar,  $10 \mu\text{m}$ .

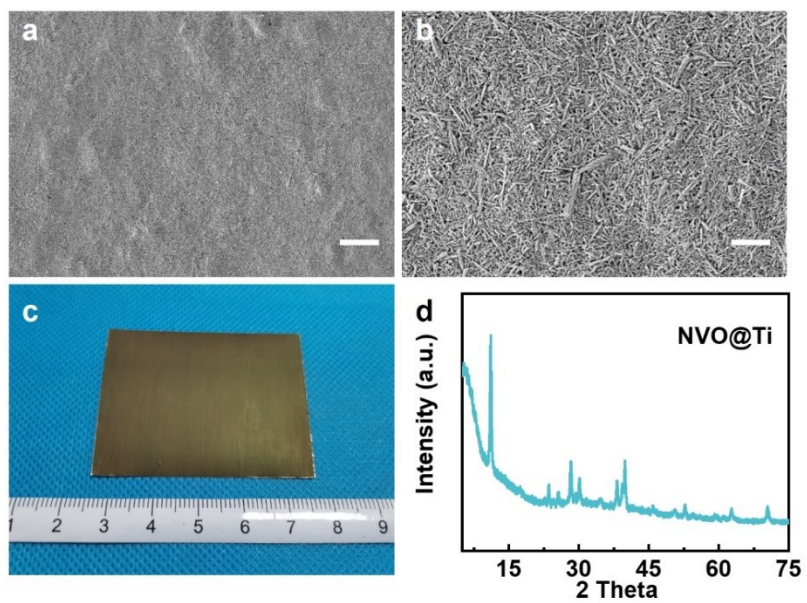


**Fig S25** (a, b) SEM images and (c) digital photo of NVO cathode ( $10 \text{ mg cm}^{-2}$ ). (d) XRD plot of NVO@Ti. Scale bar,  $10 \mu\text{m}$  for a,  $2 \mu\text{m}$  for b.

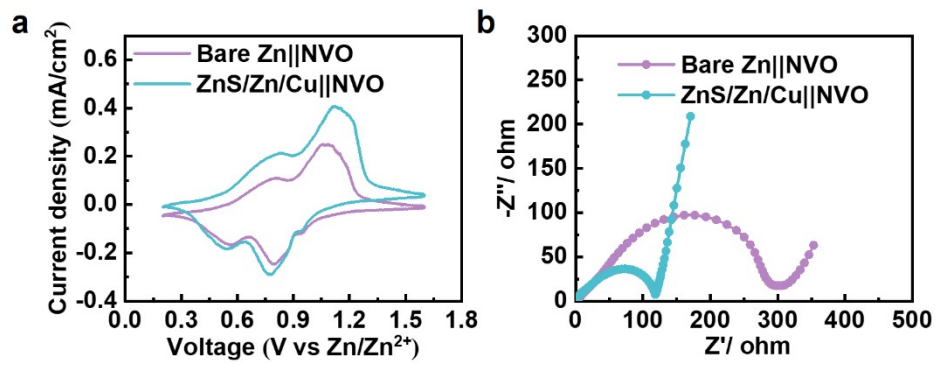


**Fig S26** (a) CV curves during the second cycle with  $0.1 \text{ mV s}^{-1}$ . (b) EIS plots of full cell.

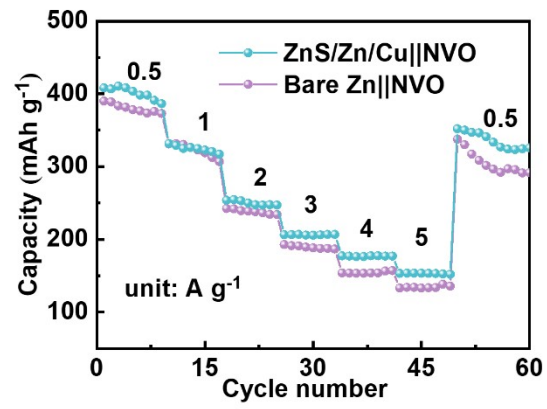
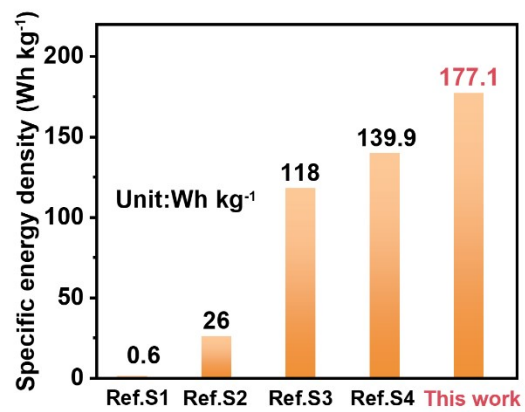
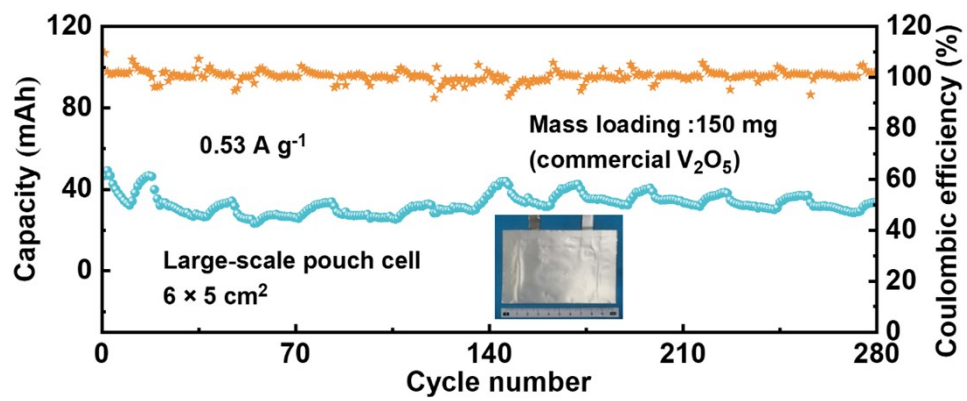


Fig S27 Rate performance of Zn||NVO and ZnS/Zn/Cu||NVO cells.



**Fig S28** Comparison of specific energy densities of full cells based on whole mass of electrodes<sup>1-4</sup>.





**Fig S29** Cycling performance of the prepared large-scale ( $6 \times 5 \text{ cm}^2$ ) pouch cell (inset is the corresponding digital image).

**Table S1.** Comparison of the asymmetric cell of this work with recent publications.

Anode	Current density (mA cm <sup>-2</sup> )	Areal capacity (mAh cm <sup>-2</sup> )	Cycle number	average CE (%)	Ref.	Year
HP-Cu  Zn	2	0.5	<b>1800</b>	<b>99.6</b>	Adv. Energy Mater. <sup>5</sup>	2023
BTO/PVT@Zn	1	0.5	<b>950</b>	<b>99.6</b>	ACS Energy Lett. <sup>6</sup>	2023
P-0.5%MXene	1	1	<b>450</b>	-	Adv. Funct. Mater. <sup>7</sup>	2023
Zn/CNT	1	0.5	<b>400</b>	<b>99.4</b>	Adv. Energy Mater. <sup>8</sup>	2023
PM@Zn	5	1	<b>400</b>	<b>98.7</b>	Angew. Chem. Int. Ed. <sup>9</sup>	2023
Zn@ZnPO	5	1	<b>927</b>	<b>99.8</b>	Adv. Funct. Mater. <sup>10</sup>	2023
Zn@DESM	2	1	<b>500</b>	<b>99.8</b>	Energy Environ. Sci. <sup>11</sup>	2023
Cflower/Zn	0.5	0.25	<b>400</b>	<b>99.3</b>	Nano. Lett. <sup>12</sup>	2023
Triple-gradient	10	1	<b>400</b>	<b>98.7</b>	Adv.Mater. <sup>13</sup>	2023
MX-TMA@Zn	2	1	<b>1000</b>	<b>99.7</b>	Energy Storage Mater. <sup>14</sup>	2022
PCu@Zn	5	1	<b>500</b>	<b>97.6</b>	Adv.Mater. <sup>15</sup>	2022
ICZ	0.5	0.5	<b>750</b>	<b>99.7</b>	Nano Energy <sup>16</sup>	2022
ZnF-Ag@Zn	1	1	<b>500</b>	<b>99.1</b>	Nano. Lett. <sup>17</sup>	2022
<b>ZnS/Zn/Cu</b>	<b>5</b>	<b>1</b>	<b>1500</b>	<b>99.9</b>	<b>This work</b>	

**Table S2.** Comparison of the symmetric cell of this work with recent publications.

Anode	Current density (mA cm <sup>-2</sup> )	Areal capacity (mAh cm <sup>-2</sup> )	Life span (h)	Cumulative capacity (mAh cm <sup>-2</sup> )	DOD (%)	Ref.
Sn@Zn-IP	2	1	700	<b>700</b>	<b>0.9</b>	Adv. Funct. Mater. <sup>18</sup>
Cu-Zn@Zn	1	3	450	<b>225</b>	<b>10.3</b>	Angew. Chem. Int. Ed. <sup>19</sup>
PC-sat	2.5	10	100	<b>125</b>	<b>68</b>	J. Am. Chem. Soc. <sup>20</sup>
Zn/Sn <sub>(200)</sub>	1	1	500	<b>250</b>	<b>1.7</b>	Adv. Mater. <sup>21</sup>
TZNC@Zn	4	4	200	<b>400</b>	<b>50</b>	Angew. Chem. Int. Ed. <sup>22</sup>
	1	1	450	<b>225</b>	<b>12.5</b>	
Zn/CNT	5	2.5	110	<b>275</b>	<b>35</b>	Adv.Mater. <sup>23</sup>
Zn Sn	1	0.5	500	<b>250</b>	<b>0.8</b>	Mater. Today Energy <sup>24</sup>
Zn@ZnF <sub>2</sub>	1	1	800	<b>400</b>	<b>1.7</b>	Adv.Mater. <sup>25</sup>
	0.5	1	500	<b>125</b>		
ZF@C-TiO <sub>2</sub>	1	1	450	<b>225</b>	<b>5</b>	Nat.Commun. <sup>26</sup>
	2	2	280	<b>280</b>	<b>10</b>	
Zn <sub>0.73</sub> Al <sub>0.27</sub> @Zn	2	2	500	<b>500</b>	<b>1.7</b>	Nano. Lett. <sup>27</sup>
Cflower/Zn	5	2.5	150	<b>375</b>	<b>1.7</b>	Nano. Lett. <sup>12</sup>
Sn@NHCF	1	1	370	<b>185</b>	<b>8</b>	Sci. Adv. <sup>28</sup>
Zn@PFSA	1	1	800	<b>400</b>	<b>5.6</b>	ACS nano <sup>29</sup>
Cu NBs@NCFs-Zn	5	2	250	<b>625</b>	<b>25</b>	Adv. Mater. <sup>30</sup>
3D Ni-Zn	5	2	200	<b>500</b>	<b>40.6</b>	Adv. Energy Mater. <sup>31</sup>
SDF	3	4.5	250	<b>375</b>	<b>45</b>	Adv. Energy Mater. <sup>32</sup>
<b>ZnS/Zn/Cu</b>	<b>5</b>	<b>5</b>	<b>300</b>	<b>750</b>	<b>85.5</b>	<b>This work</b>

**Table S3.** Comparison of the full cell of this work with recent publications.

Anode	Areal capacity (mAh cm <sup>-2</sup> )	N/P ratio	ZUR (%)	Cycles	Retention (%)
Sn@Zn-IP <sup>33</sup>	<0.1	>1100	<1	200	55
Zn@ZnPO <sup>10</sup>	0.306	191	0.5	150	90
ZBO@Zn <sup>34</sup>	4.97	2.3	43	100	60.56
HP-Zn <sup>5</sup>	1.6	3.6	30	500	41
<b>ZnS/Zn/Cu</b>	<b>4.35</b>	<b>1.34</b>	<b>74.4</b>	<b>100</b>	<b>85</b>

**Table S4.** Comparison of specific/volumetric energy densities of full cells based on Zn anodes of different thickness.

Thickness of zinc anodes	N/P ratio	Specific energy densities (Wh kg <sup>-1</sup> )	Volumetric energy densities (Wh L <sup>-1</sup> )
<b>10 μm</b>	<b>1.34</b>	<b>177.1</b>	<b>202.3</b>
50 μm	6.72	66.5	159.7
100 μm	13.4	37.3	126.5

**Supplementary description of Calculation details:**

The theoretical capacity of Zn metal is 820 mAh g<sup>-1</sup> (5855 mAh cm<sup>-3</sup>). The thickness of zinc foil is 10 μm, which provides a capacity of 5.85 mAh cm<sup>-2</sup>. In the high DOD test, the test capacity is 5 mAh cm<sup>-2</sup>.  $DOD_{85.5\%} = 5 \text{ mAh cm}^{-2} \div 5.85 \text{ mAh cm}^{-2} = 85.5\%$ . The current collector for cathode is a titanium foil with a thickness of 20 μm, the thickness of commercial separator is 20 μm, and the cathode active materials has a thickness of 100 μm (10 mg cm<sup>-2</sup>). Specific energy density is calculated based on the total mass of the electrodes, and volumetric energy density is calculated based on the entire cell volume.

## Reference

- S1. Q. Cao, Y. Gao, J. Pu, X. Zhao, Y. Wang, J. Chen and C. Guan, *Nat. Commun.*, 2023, **14**, 641.
- S2. Y. Shang, V. Kundi, I. Pal, H. N. Kim, H. Zhong, P. Kumar and D. Kundu, *Advanced Materials*, 2023, DOI: 10.1002/adma.202309212.
- S3. C. Wang, D. Wang, D. Lv, H. Peng, X. Song, J. Yang and Y. Qian, *Advanced Energy Materials*, 2023, DOI: 10.1002/aenm.202204388.
- S4. L. Yao, G. Wang, F. Zhang, X. Chi and Y. Liu, *Energy Environ. Sci.*, 2023, DOI: 10.1039/d3ee01575k.
- S5. Y. Zou, Y. Su, C. Qiao, W. Li, Z. Xue, X. Yang, M. Lu, W. Guo and J. Sun, *Adv. Energy Mater.*, 2023, **13**, 2300932.
- S6. Q. Zong, B. Lv, C. Liu, Y. Yu, Q. Kang, D. Li, Z. Zhu, D. Tao, J. Zhang, J. Wang, Q. Zhang and G. Cao, *ACS Energy Lett.*, 2023, **8**, 2886-2896.
- S7. G. Zhu, H. Zhang, J. Lu, Y. Hou, P. Liu, S. Dong, H. Pang and Y. Zhang, *Adv. Funct.l Mater.*, 2023, DOI: 10.1002/adfm.202305550.
- S8. Y. Zhou, J. Xia, J. Di, Z. Sun, L. Zhao, L. Li, Y. Wu, L. Dong, X. Wang and Q. Li, *Adv. Energy Mater.*, 2023, **13**, 2203165.
- S9. J. Zhou, Y. Mei, F. Wu, Y. Hao, W. Ma, L. Li, M. Xie and R. Chen, *Angew. Chem. Int. Ed.*, 2023, **62**, e202304454.
- S10. S. Zhang, M. Ye, Y. Zhang, Y. Tang, X. Liu and C. C. Li, *Adv. Funct.Mater.*, 2023, **33**, 2208230.
- S11. S. Zhai, W. Song, K. Jiang, X. Tan, W. Zhang, Y. Yang, W. Chen, N. Chen, H. Zeng, H. Li and Z. Li, *Energy Environ. Sci.*, 2023, DOI: 10.1039/d3ee03045h.
- S12. Z. Xu, S. Jin, N. Zhang, W. Deng, M. H. Seo and X. Wang, *Nano Lett.*, 2022, **22**, 1350-1357.
- S13. Y. Gao, Q. Cao, J. Pu, X. Zhao, G. Fu, J. Chen, Y. Wang and C. Guan, *Adv. Mater.*, 2023, **35**, e2207573.
- S14. X. Zhu, X. Li, M. L. K. Essandoh, J. Tan, Z. Cao, X. Zhang, P. Dong, P. M. Ajayan, M. Ye and J. Shen, *Energy Storage Mater.*, 2022, **50**, 243-251.
- S15. J. Zhou, F. Wu, Y. Mei, Y. Hao, L. Li, M. Xie and R. Chen, *Adv. Mater.*, 2022, **34**, e2200782.
- S16. J. Yin, Y. Wang, Y. Zhu, J. Jin, C. Chen, Y. Yuan, Z. Bayhan, N. Salah, N. A. Alhebshi, W. Zhang, U. Schwingenschlögl and H. N. Alshareef, *Nano Energy*, 2022, **99**, 107331.
- S17. D. Wang, D. Lv, H. Peng, N. Wang, H. Liu, J. Yang and Y. Qian, *Nano Lett.*, 2022, **22**, 1750-1758.
- S18. Q. Cao, Z. Pan, Y. Gao, J. Pu, G. Fu, G. Cheng and C. Guan, *Adv. Funct. Mater.*, 2022, **32**, 2205771.
- S19. B. Li, K. Yang, J. Ma, P. Shi, L. Chen, C. Chen, X. Hong, X. Cheng, M. C. Tang, Y. B. He and F. Kang, *Angew. Chem. Int. Ed.*, 2022, **61**, e202212587.
- S20. F. Ming, Y. Zhu, G. Huang, A.-H. Emwas, H. Liang, Y. Cui and H. N. Alshareef, *J. Am. Chem. Soc.*, 2022, **144**, 7160-7170.
- S21. S. Li, J. Fu, G. Miao, S. Wang, W. Zhao, Z. Wu, Y. Zhang and X. Yang, *Adv. Mater.*, 2021, **33**, 2008424.
- S22. P. X. Sun, Z. Cao, Y. X. Zeng, W. W. Xie, N. W. Li, D. Luan, S. Yang, L. Yu and X. W. D. Lou, *Angew. Chem. Int. Ed.*, 2022, **61**, e202115649.
- S23. Y. Zeng, X. Zhang, R. Qin, X. Liu, P. Fang, D. Zheng, Y. Tong and X. Lu, *Adv. Mater.*, 2019, **31**, e1903675.
- S24. W. Guo, Y. Zhang, X. Tong, X. Wang, L. Zhang, X. Xia and J. Tu, *Mater. Today Energy*, 2021, **20**, 100675.
- S25. Y. Yang, C. Liu, Z. Lv, H. Yang, Y. Zhang, M. Ye, L. Chen, J. Zhao and C. C. Li, *Adv. Mater.*, 2021, **33**, e2007388.
- S26. Q. Zhang, J. Luan, X. Huang, Q. Wang, D. Sun, Y. Tang, X. Ji and H. Wang, *Nat. Commun.*, 2020, **11**, 3961.
- S27. J. Zheng, Z. Huang, Y. Zeng, W. Liu, B. Wei, Z. Qi, Z. Wang, C. Xia and H. Liang, *Nano Lett.*, 2022, **22**, 1017-1023.
- S28. H. Yu, Y. Zeng, N. W. Li, D. Luan, L. Yu and X. W. D. Lou, *Sci. Adv.*, 2022, **8**, eabm5766.
- S29. L. Hong, X. Wu, L.-Y. Wang, M. Zhong, P. Zhang, L. Jiang, W. Huang, Y. Wang, K.-X. Wang and J.-S. Chen, *ACS Nano*, 2022, **16**, 6906-6915.

- S30. Y. Zeng, P. X. Sun, Z. Pei, Q. Jin, X. Zhang, L. Yu and X. W. David Lou, *Adv. Mater.*, 2022, **34**, 2200342.
- S31. G. Zhang, X. Zhang, H. Liu, J. Li, Y. Chen and H. Duan, *Adv. Energy Mater.*, 2021, **11**, 2003927.
- S32. Z. Shen, L. Luo, C. Li, J. Pu, J. Xie, L. Wang, Z. Huai, Z. Dai, Y. Yao and G. Hong, *Adv. Energy Mater.*, 2021, **11**, 2100214.
- S33. Q. H. Cao, Z. H. Pan, Y. Gao, J. Pu, G. Fu, G. Cheng and C. Guan, *Adv. Funct. Mater.*, 2022, **32**.
- S34. D. Wang, H. Liu, D. Lv, C. Wang, J. Yang and Y. Qian, *Adv. Mater.*, 2022, **35**, 2207908.